

# Solar models with new low-metal abundances

Wuming Yang

*Department of Astronomy, Beijing Normal University, Beijing 100875, China*

yangwuming@bnu.edu.cn; yangwuming@ynao.ac.cn

## ABSTRACT

In the last decade, the photospheric abundances of the Sun had been revised several times by many observers. The standard solar models (SSM) constructed with the new low-metal abundances disagree with helioseismic results and detected neutrino fluxes. The solar model problem has been puzzled some stellar physicists for more than ten years. Rotation, enhanced diffusion, convection overshoot, and magnetic fields are used to reconcile the new abundances with helioseismology. The **too** low-helium **subsurface abundance** in enhanced diffusion models can be improved by the mixing caused by rotation and magnetic fields. The problem of the depth of the convective zone in rotating models can be resolved by convection overshoot. Consequently the Asplund-Grevesse-Sauval rotation model including overshooting (AGSR) reproduces the seismically inferred sound-speed and density profiles, and the convection zone depth as well as the Grevesse and Sauval (GS98) model computed before. But this model fails to reproduce the surface helium abundance which is  $0.2393$  ( $2.6 \sigma$  away from the seismic value) and neutrino fluxes. The magnetic model called AGSM keeps the agreement of the AGSR and improves the prediction of the surface helium abundance. The observed separation ratios  $r_{02}$  and  $r_{13}$  are reasonably reproduced by AGSM. Moreover, neutrino fluxes calculated by this model are not far from the detected neutrino fluxes and the predictions of previous works.

*Subject headings:* Sun: abundances — Sun: helioseismology — Sun: interiors — Sun: magnetic fields — Sun: rotation

## 1. Introduction

### 1.1. The constraints of helioseismology

Since Lodders (2003) and Asplund et al. (2004, 2005) revised the ratio of heavy-element abundance to hydrogen abundance of the Sun ( $Z/X$ ) from the old 0.023 (Grevesse & Sauval 1998, hereafter GS98) to 0.0177 (Lodders 2003) or 0.0165 (Asplund et al. 2005, hereafter AGS05), the solar model problem (or the solar abundance problem) that standard solar models (SSM) constructed with the AGS05 mixtures disagree with the seismically inferred sound-speed and density profiles, convection zone (CZ) depth, and CZ helium abundance has been perplexed some solar physicists, see Turck-Chièze et al. (2004). The seismically inferred CZ base radius is  $0.713 \pm 0.003 R_{\odot}$  (Christensen-Dalsgaard et al. 1991) or  $0.713 \pm$

$0.001 R_{\odot}$  (Basu & Antia 1997), and CZ helium abundance is  $0.2485 \pm 0.0035$  (Basu & Antia 2004; Serenelli & Basu 2010).

Many models have been proposed to resolve the problem. It was found that a 11%–20% increase in OPAL opacities at the base of the CZ (BCZ) can reconcile the low-Z models with helioseismology (Basu & Antia 2004; Montalbán et al. 2004; Bahcall et al. 2004). However, Badnell et al. (2005) and Guzik et al. (2005) showed that the increase in the opacities is no more than about 3.0% near the BCZ. Antia & Basu (2005) and Bahcall et al. (2005) found that an increase in neon abundance along with small increases in the other abundances could solve the problem with AGS05 models. However, Schmelz et al. (2005) and Young (2005) showed that the Ne/O ratio is indeed consistent with the value given by AGS05. Asplund et al. (2004) suggested that in-

creased diffusion and settling of helium and heavy elements might be able to resolve these disagreements. Several groups, e.g., Basu & Antia (2004), Montalbán et al. (2004), Guzik et al. (2005), and Yang & Bi (2007) considered the effects of enhanced diffusion. They found that enhanced diffusion depletes the CZ helium abundance to well below the seismically inferred value and leaves the position of the BCZ too shallow.

Recently, Lodders (2009), Asplund et al. (2009), and Caffau et al. (2010) reevaluated the spectroscopic abundances of the Sun. The heavy-element abundance was revised to  $Z/X = 0.0181$  and  $Z = 0.0134$  (Asplund et al. 2009, hereafter AGS09),  $Z/X = 0.0191$  and  $Z = 0.0141$  (Lodders 2009), and  $Z/X = 0.0211$  and  $Z = 0.0154$  (Caffau et al. 2010). Compared to the SSMs with GS98 mixtures, solar models constructed in accordance to the AGS09 mixtures also disagree with the seismically inferred sound-speed and density profiles, CZ depth, and CZ helium abundance (Serenelli et al. 2009; Serenelli & Basu 2010; Serenelli et al. 2011; Guzik et al. 2010; Bi et al. 2011; Turck-Chièze et al. 2010, 2011; Lopes & Turck-Chièze 2013, 2014; Le Pennec et al. 2015). The conclusion has been that it is difficult to match simultaneously the new  $Z/X$  and helioseismic constraints for sound-speed and density profiles, CZ depth, and CZ helium abundance. A resolution to the solar model problem remains elusive.

The hypothesis of a large error in the new photospheric abundance estimate has now been ruled out (Lodders 2009; Asplund et al. 2009; Caffau et al. 2010). Assuming accretion of metal-poor gas at the beginning of the main sequence of the Sun, Castro et al. (2007), Guzik et al. (2010), and Serenelli et al. (2011) found that the sound-speed profile of accretion model matches very well that of the GS98 SSM below  $R/R_{\odot} = 0.5$ , but the bump below the CZ remains quite prominent. Furthermore, the CZ depth of the accretion model is too shallow. Moreover, Serenelli et al. (2011) considered accretion of metal-rich gas. Metal-rich accretion can bring the depth of the CZ into agreement with the seismic value, but that the resulting surface He abundance in such models is too low.

The effects of a convective overshoot were considered by Montalbán et al. (2006), Castro et al. (2007), and Guzik et al. (2010). The overshoot

below the CZ allows Montalbán et al. (2006) and Castro et al. (2007) to recover the good CZ radius but can not improve sound-speed and surface He abundance (Montalbán et al. 2006; Castro et al. 2007; Guzik et al. 2010). Moreover, the CZ radius of overshoot model of Guzik et al. (2010) is not in agreement with the seismic value; and the effects of a convective overshoot does not inhibit He diffusion (Guzik et al. 2010). Guzik et al. (2010) also considered the effects of mass loss. They found that the sound-speed agreement is considerably improved by including early mass loss. But the CZ depth is still too low.

Turck-Chièze et al. (2010) constructed dynamical solar models including a detailed transport of angular momentum and chemicals due to internal rotation that includes meridional circulation and shear-induced turbulence. They found that the impact of the rotation on the solar structure is rather small, and the sound speed is only very slightly modified when internal rotation is introduced with respect to the measured internal rotation profile. Their work sustains the idea that the Sun was not at the beginning a rapid rotator, and that other dynamical processes should be included to better reproduce the observed solar profile and to better describe the young active Sun. Furthermore, Turck-Chièze et al. (2011) concluded that about 20% of the present discrepancy could come from the incorrect description of the early phase of the Sun, its activity, its initial mass, and mass-loss history. Turck-Chièze et al. (2011) also found that the solar initial mass could have been larger by 20%–30% than the present solar mass, and that the Sun could have transformed about 2.5% – 4% of the energy produced during the early evolutionary stages into other form of energy through kinetic and magnetic energies. Turck-Chièze et al. (2011) put forward an important view that a transformation of nuclear energy into kinetic and magnetic energies during the solar life must be considered. Zhang (2014) found that the density profile below the CZ is sensitive to the turbulent kinetic flux, which supports the view of Turck-Chièze et al. (2011).

Moreover, Le Pennec et al. (2015) constructed a standard solar model with the new OPAS opacity tables. Their results show that OPAS opacities improve the sound-speed profile but the bump below the CZ remains quite prominent (see their

Figures 3 and 4).

## 1.2. The neutrino flux constraints

In the last decade, important progress has been made in the **detection of neutrinos** (Ahmed et al. 2004; Bellini et al. 2011, 2012) and in the **prediction of solar neutrino fluxes** (Turck-Chièze et al. 2001, 2004, 2010; Turck-Chièze & Couvidat 2011; Turck-Chièze & Lopes 2012; Bahcall et al. 2001; Bahcall & Pinsonneault 2004; Couvidat et al. 2003; Lopes & Turck-Chièze 2013, 2014). The Sudbury Neutrino Observatory confirmed the existence of solar neutrino oscillations (Ahmed et al. 2004). The  $^8\text{B}$ ,  $^7\text{Be}$ ,  $pp$ , and  $pep$  neutrino fluxes were determined (Ahmed et al. 2004; Bellini et al. 2011, 2012).

Seismic observations constrain mainly the external layers of the **Sun and the internal seismic sound speed**, but neutrino fluxes probe the real center of the Sun. Neutrinos have complemented helioseismology in diagnosing the structure of the Sun (Turck-Chièze et al. 2011; Turck-Chièze & Lopes 2012). The boron neutrino flux is strongly dependent on solar central temperature (Couvidat et al. 2003; Turck-Chièze et al. 2010; Turck-Chièze & Lopes 2012). The  $pep$  neutrino flux is dramatically dependent on the luminosity of the Sun. Therefore, it represents a powerful probe of the physics of the nuclear region of the Sun, in parallel to the information introduced in the seismic model (Turck-Chièze & Lopes 2012; Lopes & Turck-Chièze 2013). Thus neutrinos provide a direct constraint on the solar core, see the review of Turck-Chièze & Couvidat (2011).

The solar neutrinos have been used to diagnose the temperature profile in the Sun's core, measure the radial electronic density of matter of the Sun (Turck-Chièze & Lopes 2012; Lopes & Turck-Chièze 2013) and the strength of magnetic field in the radiative region (Couvidat et al. 2003), and look for standing g-modes of the Sun (Lopes & Turck-Chièze 2014).

## 1.3. The uncertainties on the elemental diffusion and mixing

The rates of element diffusion are enhanced by applying a straight multiplier to the diffusion velocity, as has been done by Basu & Antia (2004), Montalbán et al. (2004), Guzik et al. (2005), and

Yang & Bi (2007). The theoretical error of the gravitational settling rate is of the order of about 15% (Thoul, Bahcall & Loeb 1994). Our multipliers of the diffusion coefficients are very high, despite the fact that there is no obvious physical justification for such high multipliers, as has been pointed out by Basu & Antia (2004) and Guzik et al. (2005).

Gravitational settling reduces the surface helium abundance by roughly 10% ( $\approx 0.03$  by mass fraction) below its initial value but this estimate is still subjected to great uncertainties (Proffitt & Michaud 1991). Thoul, Bahcall & Loeb (1994) find the same order of magnitude but state that the effects of meridional circulation and of turbulent mixing are ignored in their models. Proffitt & Michaud (1991) estimated the effect of turbulent mixing on gravitational settling. They found that turbulent mixing could partly inhibit the settling of helium by about 40%. Their turbulent diffusion coefficient is very different from those given by Pinsonneault et al. (1989) and Zahn et al. (1997). Proffitt & Michaud (1991) concluded that it is unlikely that turbulent mixing of any kind can reduce the amount of surface He settling in solar models by more than a factor of 2 below that calculated for pure diffusion models. Turck-Chièze et al. (2010) **finds that rotational mixing has a limited effect on the diffusion for realistic internal rotation rate.**

The observed subsurface mass fraction of helium is  $0.2485 \pm 0.035$  (Basu & Antia 2004). As the initial helium abundance of the Sun varies between  $0.273 \pm 0.006$  and  $0.278 \pm 0.006$  (Serenelli & Basu 2010), the roughly 10% reduction in the surface helium abundance is generally required in many best solar models, such as BP00 (Bahcall et al. 2001), BP04 (Bahcall & Pinsonneault 2004), and SSeM (Couvidat et al. 2003), to reproduce seismic results. So, in order to keep such surface helium abundance, the rate of element diffusion must be enhanced in our rotating models. Guzik et al. (2005), Basu & Antia (2008), Turck-Chièze et al. (2011) and Le Penec et al. (2015) also pointed out that there may be an insufficient treatment of the microscopic diffusion.

In order to restore agreement between seismic constraints and models that are constructed with the AGS09 abundances, based on the rotating models of Pinsonneault et al. (1989) and

Yang & Bi (2007), the combinations of diffusion, rotation, convection overshoot, and magnetic fields are considered in this work.

The effects of rotation on the structure and evolution of stars include centrifugal effect and rotational mixing (Pinsonneault et al. 1989; Yang & Bi 2006; Turck-Chièze et al. 2010; Yang et al. 2013a,b). The mechanisms of rotational mixing, considered in this work, include the hydrodynamical instabilities (Pinsonneault et al. 1989) and secular shear instability (Zahn et al. 1997).

The overshoot of convection extends the region of chemical mixing by a distance  $\delta_{ov}H_p$  below the BCZ that is determined by Schwarzschild criterion, where  $H_p$  is the local pressure scaleheight and  $\delta_{ov}$  is a free parameter. The full mixing of chemical compositions is assumed in the overshoot region in our models. The paper is organized as follow: the properties of the different solar models are presented in section 2, results are given in section 3, a discussion and summary in section 4.

## 2. Proposed Solar Models

The solar models are computed by using Yale Rotation Evolution Code (Pinsonneault et al. 1989; Guenther et al. 1992; Yang & Bi 2007) in its rotation and non-rotation configurations. The OPAL equation-of-state (EOS2005) tables (Rogers & Nayfonov 2002) and OPAL opacity tables (Iglesias & Rogers 1996) were used, supplemented by the Ferguson et al. (2005) opacity tables at low temperature. The opacity tables were reconstructed using GS98 or AGS09 mixtures. The low-temperature opacity tables with AGS09 mixtures were computed by Ferguson for Serenelli et al. (2009). Convection is treated according to the standard mixing-length theory. The diffusion and settling of both helium and heavy elements are computed by using the diffusion coefficients of Thoul, Bahcall & Loeb (1994). All models are calibrated to the present solar radius  $6.9598 \times 10^{10}$  cm, luminosity  $3.844 \times 10^{33}$  erg s<sup>-1</sup>, mass  $1.9891 \times 10^{30}$  g, and age 4.57 Gyr. The initial  $X_{init}$  and  $Z_{init}$ , and mixing-length parameter  $\alpha$  are adjusted to match the constraints of luminosity and radius within about  $10^{-4}$ . The values of the parameters are summarized in Table 1.

The nuclear reaction rates were evaluated with the subroutine of Bahcall & Pinsonneault

(1992), updated by Bahcall et al. (1995) and Bahcall et al. (2001) using the reaction data in Adelberger et al. (1998), Gruzinov & Bahcall (1998), and Marcucci et al. (2000).

Following Li & Sofia (2001), we use the toroidal ( $B_t$ ) and poloidal ( $B_p$ ) components to express a magnetic field vector  $\mathbf{B} = (B_t, B_p)$ . We assume  $|B_t| \gg |B_p|$  in the radiative region. The magnetic energy density variable  $\chi$  is defined as

$$\chi = (B^2/8\pi)/\rho, \quad (1)$$

where  $B = (B_t^2 + B_p^2)^{1/2}$  is the magnitude of the magnetic field vector. The magnetic pressure  $P_\chi$  can be written as

$$P_\chi = \chi\rho. \quad (2)$$

The total pressure  $P_T$  is written as

$$P_T = P + P_\chi. \quad (3)$$

The equation of state becomes

$$\frac{d\rho}{\rho} = \alpha \frac{dP_T}{P_T} - \delta \frac{dT}{T} - \psi \frac{d\chi}{\chi}, \quad (4)$$

where

$$\alpha = \left(\frac{\partial \ln \rho}{\partial \ln P_T}\right)_{T,\chi}, \delta = -\left(\frac{\partial \ln \rho}{\partial \ln T}\right)_{P_T,\chi}, \psi = -\left(\frac{\partial \ln \rho}{\partial \ln \chi}\right)_{P_T,T}. \quad (5)$$

The energy conservation equation becomes

$$\frac{\partial L}{\partial M_r} = \epsilon - T \frac{dS_T}{dt}, \quad (6)$$

where

$$T dS_T = dU + PdV + d\chi \quad (7)$$

is the first law of thermodynamics including magnetic fields (Li & Sofia 2001). The total internal energy  $U_T = U + \chi$  and the total entropy  $S_T = S + \chi/T$ .

The transport process of angular momentum and chemical compositions caused by magnetic fields is treated as a diffusion process, i.e.,

$$\frac{\partial \Omega}{\partial t} = f_\Omega \frac{1}{\rho r^4} \frac{\partial}{\partial r} (\rho r^4 D_m \frac{\partial \Omega}{\partial r}), \quad (8)$$

$$\frac{\partial X_i}{\partial t} = f_c f_\Omega \frac{1}{\rho r^2} \frac{\partial}{\partial r} (\rho r^2 D_m \frac{\partial X_i}{\partial r}), \quad (9)$$

where  $D_m = r^2 \Omega B_p^2 / B^2$  is the diffusion coefficient,  $f_\Omega$  and  $f_c$  are a constant between

0 and 1 (Yang & Bi 2006, 2008), respectively. The strength and spatiotemporal distribution of magnetic fields inside a star are poorly known. Yang & Bi (2006) assumed that  $B_p^2/B^2$  is a constant. Due to  $|B_t| \gg |B_p|$ , here we take  $|B| \approx |B_t|$ . The magnetic field compositions  $|B_t|$  and  $|B_p|$  in the radiative region are calculated by using equations (22) and (23) of Spruit (2002). The values of  $f_\Omega$  and  $f_c$  are shown in Table 1.

Solid body rotation is assumed in the CZ. And the distribution of the magnitude of magnetic fields is assumed to be a Gaussian profile (Li & Sofia 2001) in the CZ, i.e.,

$$B = B_{BCZ} \exp[-\frac{1}{2}(r - r_{BCZ})^2/\sigma^2], \quad (10)$$

where the  $B_{BCZ}$  is determined by the equations of Spruit (2002). The magnitude of  $B_{BCZ}$  is of the order of about  $2 \times 10^3$  Gauss. The value of the  $\sigma$  is equal to 0.05. With these assumptions, the magnitude of magnetic fields is about 1 Gauss at  $M_r/M_\odot = 0.9998$ . Our model is a simplified representation of the convective magnetic field. Our simple description does not respect the stability and specific configuration of magnetic fields. Duez et al. (2009, 2010) studied the impact of large-scale magnetic fields on the structure and evolution of stars. They pointed out that a mixed poloidal-toroidal configuration is needed for the fields to survive over evolution timescales.

We constructed the following five models: 1) GS98M, a standard solar model constructed by using GS98 mixture opacities; 2) AGS1, a standard model with AGS09 mixture opacities; 3) AGS2, an enhanced diffusion model with AGS09 mixture opacities; 4) AGSR, same as AGS2 but with rotation (Pinsonneault et al. 1989; Yang & Bi 2007) and convection overshoot; 5) AGSM, same as AGSR but including the effects of magnetic fields. The initial rotation velocity  $V_{init}$  of models is a free parameter and is adjusted to obtain the surface rotation velocity of about  $2.0 \text{ km s}^{-1}$  at the age of 4.57 Gyr. The values of the parameters of diffusion and convection overshoot are shown in Table 1.

### 3. Calculation Results

#### 3.1. Standard and enhanced diffusion models

The sound speed and density of our ad hoc models are compared to those inferred in Basu et al. (2009) using Birmingham Solar-Oscillations Network (BiSON) (Chaplin et al. 1996) data. The position of the CZ base, the surface helium abundance and heavy-element abundance of the models are listed in Table 1. Compared to the seismically inferred CZ base radius (Basu & Antia 1997) and helium abundance (Basu & Antia 2004), the position of the CZ base of AGS1 is too shallow and its surface helium abundance is too low. Figures 1 and 2 show the relative differences between the calculated and inferred sound speed and density profiles. The relative sound-speed and density differences of AGS1 are too large compared to those of GS98M, as has been shown by many authors (Serenelli et al. 2009; Serenelli & Basu 2010; Serenelli et al. 2011; Guzik et al. 2010; Bi et al. 2011; Turck-Chièze et al. 2010, 2011; Le Pennec et al. 2015).

In order to obtain the model that can restore agreement with helioseismology, we constructed the models with an enhanced diffusion rate, following Basu & Antia (2004), Guzik et al. (2005), and Yang & Bi (2007). However, we have no physical justification for these multipliers that are required to restore agreement with helioseismology in our calculations. Due to the effect of the enhanced diffusion, radial distributions of element abundances of AGS2 are closer to those of GS98M in the radiative region than those of AGS1 (see Figure 3). Thus the CZ base radius, the sound-speed and density profiles of AGS2 are close to those of GS98M. However, the surface helium abundance of 0.223 is  $6 \sigma$  away from the seismically inferred value (Basu & Antia 2004).

#### 3.2. Rotating model

Rotational and turbulent mixing can reduce the surface helium settling (Proffitt & Michaud 1991; Yang & Bi 2006; Turck-Chièze et al. 2010; Yang et al. 2013a,b). But the position of the CZ base of rotating models with low Z is too shallow (Yang & Bi 2007). Montalbán et al. (2006) and Castro et al. (2007) showed that convective over-

shoot can bring the depth of the CZ into agreement with the seismic value. Therefore, in order to resolve the low-helium problem and the CZ depth problem, we constructed rotating solar model AGSR with a convection overshoot that is described by parameter  $\delta_{ov}$ . The convection overshoot brings the CZ base radius into agreement with the seismic value. By full mixing the material in the overshoot region with that in the convective envelope, convection overshoot should lead to an increase in the surface helium abundance. The mass of overshoot region for  $\delta_{ov} = 0.1$  or  $0.2$  is about  $0.1\% - 0.2\% M_{\odot}$ , but the mass of the CZ is around  $2.5\% M_{\odot}$ . Moreover, the gradient of helium abundance at the base of the convective envelope, caused by microscopic diffusion and element settling, has been partly flattened by rotational mixing. Thus the increase in helium abundance caused by the overshooting is very small. Compared with the effect of rotational mixing, the effect of the overshooting on the surface helium abundance is negligible. The convection overshoot does not improve the surface helium abundance.

Due to the fact that rotational velocity is low, centrifugal effect is negligible in AGSR. The impact of rotation on the solar model mainly derives from the effects of rotational mixing that rely on hydrodynamical instabilities considered in the model. The initial element abundances of AGSR are almost the same as those of AGS2. Figure 3 shows that rotational mixing considered in AGSR do not affect clearly the distributions of element abundances below  $0.5 R_{\odot}$ . Thus the models AGS2 and AGSR have almost the same central temperature, density, element abundances (see Table 1), and neutrino fluxes (see Table 2). However, the rotational mixing below the CZ base partly counteracts the surface He and heavy-element settling. Therefore, the He and heavy-element abundances of AGSR are higher than those of AGS2 above  $0.65 R_{\odot}$  but are lower than those of AGS2 between about  $0.5$  and  $0.65 R_{\odot}$ . So the density of AGSR is larger than that of AGS2 above  $0.65 R_{\odot}$  but is smaller than that of AGS2 between about  $0.5$  and  $0.65 R_{\odot}$ . As a consequence, the sound-speed profile of AGSR is significantly changed between about  $0.5$  and  $0.7 R_{\odot}$ .

Rotational mixing in AGSR reduces the amount of surface He settling by about 29% and the amount of surface heavy element settling by about

5%. Although the rate of element diffusion is multiplied by a factor of 2 for helium abundance, the surface helium abundance is reduced by only about 14% below its initial value in AGSR.

The CZ base radius of  $0.714 R_{\odot}$  of AGSR is consistent with the seismically inferred value of  $0.713 \pm 0.001 R_{\odot}$  (Basu & Antia 1997). The absolute values of relative sound-speed difference,  $\delta c/c$ , and density difference,  $\delta\rho/\rho$ , between AGSR and the Sun are less than 0.0035 and 0.016, respectively. These values are slightly less than those of GS98M. The density profile of AGSR is better than that of GS98M. The surface helium abundance of 0.23928 of AGSR is in agreement with the seismically inferred value at the level of  $2.6 \sigma$ .

However, Figure 4 shows that the frequencies of low-degree p-modes of AGSR are not as good as those of GS98M. Neutrino fluxes calculated from AGSR disagree with those predicted by Couvidat et al. (2003), Turck-Chièze et al. (2004), and Bahcall & Pinsonneault (2004).

### 3.3. Rotating model including the effects of magnetic fields

Turck-Chièze et al. (2010, 2011) suggested that magnetic fields should be considered in solar models. The effects of magnetic pressure, magnetic energy, and the mixing of angular momentum and chemical compositions caused by magnetic fields are considered in AGSM.

Compared with the effect of rotational and magnetic mixing, the effect of the overshooting on the surface helium abundance is negligible in AGSM. But the convection overshoot allows us to recover the CZ base radius at the level of  $1\sigma$ . The surface He abundance is 0.2445, which agrees with seismic value at the level of  $1.1\sigma$ . The surface Z/X ratio of this model is 0.0187. The mixing caused by rotation and magnetic fields efficiently reduces the surface He settling. Thus the He abundance of AGSM is higher than that of AGSR above  $0.63 R_{\odot}$  but is lower than that of AGSR below  $0.63 R_{\odot}$ . The mixing reduces the amount of surface He settling by about 47% in AGSM, which is slightly higher than 40% that was obtained by Proffitt & Michaud (1991) using different diffusion coefficient but does not exceed the upper limit of 50% assumed by Proffitt & Michaud (1991). The surface He abundance is reduced by only 11%

( $\approx 0.03$  by mass fraction) below its initial value. Although the rate of element diffusion is multiplied by a factor of 2 for helium abundance, the 11% reduction in the surface He abundance is consistent with that of GS98M.

The relative sound-speed difference and density difference between AGSM and the Sun,  $\delta c/c$  and  $\delta\rho/\rho$ , are less than 0.0058 and 0.019, respectively. The density profile of AGSM is as good as that of GS98M (see Figure 2). The bump of sound-speed profile mainly appears between 0.63 and 0.71  $R_\odot$ . Between 0.1 and 0.6  $R_\odot$ , the sound speed and density of this model match very well with those inferred by Basu et al. (2009).

Figure 4 represents the differences between observed frequencies of low-degree p-modes (García et al. 2011) and those calculated from different models, which shows that the agreement between the observed and theoretical frequencies is improved by the effects of magnetic fields.

The initial rotation velocity of AGSR and AGSM is  $5.8 \text{ km s}^{-1}$ , which is consistent with the conclusion that solar rotation velocity is in the range of  $5 - 10 \text{ km s}^{-1}$  at zero-age main sequence (Turck-Chièze et al. 2010). The surface velocity of both AGSR and AGSM is about  $2 \text{ km s}^{-1}$ . Efficient transport of angular momentum flattens the angular velocity profile of AGSM between about 0.3 and 0.7  $R_\odot$  (see Figure 5), which is consistent with seismically inferred result (Chaplin et al. 1999a) and is compatible with the first observation of gravity modes (see figures 2 and 4 of García et al. (2007) or figure 8 of Turck-Chièze et al. (2010)). The central angular velocity is 5 times as large as the surface angular velocity. The total angular momentum of AGSM is  $2.40 \times 10^{48} \text{ g cm}^2 \text{ s}^{-1}$  that is closer to  $1.94 \pm 0.05 \times 10^{48} \text{ g cm}^2 \text{ s}^{-1}$  inferred by Komm et al. (2003) than  $3.85 \times 10^{48} \text{ g cm}^2 \text{ s}^{-1}$  of AGSR.

The magnetic energy is mainly stored in the radiative region (see Figure 5). Couvidat et al. (2003) showed that an internal large-scale magnetic field cannot exceed a maximum strength of about  $3 \times 10^7 \text{ G}$  in the radiative region. The strength of magnetic field of AGSM is less than about  $3 \times 10^4 \text{ G}$  in the radiative region but is less than around  $3 \times 10^3 \text{ G}$  in the CZ.

Furthermore, Figures 6 and 7 show the distri-

butions of ratios of small to large separations,  $r_{02}$  and  $r_{13}$ , of these models as a function of frequency. The ratios are essentially independent of the structure of outer layer and are only determined by the interior structure of stars (Roxburgh & Vorontsov 2003). The distributions of the ratios of AGS1 disagree with those calculated from the observed frequencies of Chaplin et al. (1999b) or García et al. (2011). This indicates that interior structures of AGS1 do not match those of the Sun. Although the GS98M model performs much better than other models, the observed ratios are almost reproduced by AGSR and AGSM.

### 3.4. Prediction of neutrino fluxes

Neutrino fluxes can provide a strict constraint on the core of the Sun, which is independent on helioseismology (Turck-Chièze & Couvidat 2011). Table 2 lists detected and predicted solar neutrino fluxes. The BP04 and SSeM are the best model of Bahcall & Pinsonneault (2004), Couvidat et al. (2003) and **Turck-Chièze et al. (2011)**, respectively. These models not only are in agreement with helioseismic results, but can reproduce the measured neutrino fluxes (Bahcall & Pinsonneault 2004; Turck-Chièze et al. 2001, 2004, 2010, 2011; Couvidat et al. 2003; Turck-Chièze & Couvidat 2011). We compare neutrino fluxes computed from our models with those predicted by BP04 and SSeM.

The neutrino fluxes calculated from GS98M are in good agreement with those predicted by Bahcall et al. (2001) except  ${}^7\text{Be}$  neutrino flux. The  ${}^7\text{Be}$  neutrino flux computed from GS98M is also larger than those predicted by BP04 and SSeM. The neutrino fluxes calculated from AGS1, AGS2, and AGSR are obviously different from those predicted by GS98M, BP04, and SSeM. However, the fluxes of  $pp$ ,  $pep$ ,  ${}^8\text{B}$ ,  ${}^{13}\text{N}$ , and  ${}^{15}\text{O}$  neutrinos of AGSM are almost in agreement with those of BP04 (Bahcall & Pinsonneault 2004) and SSeM (Turck-Chièze et al. 2001, 2004, 2011; Couvidat et al. 2003; Turck-Chièze & Couvidat 2011). The  ${}^{17}\text{F}$  neutrino flux of AGSM is also in agreement with that of BP04 but is higher than that of SSeM. The relative difference between the neutrino fluxes of AGSM and those of BP04 is less than 2.0%.

The  $hep$  neutrino flux of AGSM is consistent with those of GS98M but is higher than that of

BP04. The discrepancy between *hep* neutrino flux of AGSM and that of BP04 can be attributed to the nuclear cross section factor  $S_0(\text{hep})$  which only affects the flux of *hep* neutrinos and does not affect the calculated fluxes of other neutrinos (Bahcall et al. 2001). Comparing the neutrino fluxes calculated from AGS1, AGS2, AGSR, and AGSM with those predicted by BP04 and SSeM and the detected neutrino fluxes, one can find that the neutrino-flux agreement is considerably improved by the effects of magnetic fields and that AGSM is obviously better than **pure SSM** low-Z models.

#### 4. Discussion and Summary

The equatorial velocity of about  $2 \text{ km s}^{-1}$ , i.e.  $2.94 \times 10^{-6} \text{ rad s}^{-1}$ , is taken as the surface velocity of models at the age of the Sun. **This value** is slightly higher than  $2.72 \times 10^{-6} \text{ rad s}^{-1}$  adopted by Komm et al. (2003). Thus the total angular momentum of AGSM is slightly larger than that inferred by Komm et al. (2003). The low angular velocity can be achieved by a slow initial rotation. The sound speed profile is practically unchanged when a slower initial rotation is adopted, which is consistent with the result of Turck-Chièze et al. (2010).

The rates of element diffusion are enhanced by multiplying a factor of 2 to the diffusion velocity of He and a factor of 2.5 to the diffusion velocity of heavy elements. The effect of mixing caused by rotation and magnetic fields reduces the amount of surface He settling by about 47%. So the surface He abundance is reduced by only 11% below its initial value. A roughly 10% reduction in the surface He abundance has been proved by many best solar models. Solar activity and helioseismology show the limitation of SSM and call for the dynamical solar model including dynamical processes (Turck-Chièze et al. 2010; Turck-Chièze & Couvidat 2011). In order to keep a roughly 10% reduction in the surface He abundance, the rates of element diffusion must be enhanced in our dynamical solar models.

The SSM with AGS09 mixtures does not agree with seismic constraints for sound-speed and density profiles, CZ base radius, and CZ helium abundance. Thus we calculated the dynamical solar models that include the effects of enhanced dif-

fusion, rotation, convection overshoot, and magnetic fields. The discrepancies between models with AGS09 mixtures and helioseismic results can be significantly reduced by the enhanced diffusion. However, the surface helium abundance of the enhanced diffusion model is too low. The surface He settling can be partially counteracted by rotational mixing. Thus the low-helium problem can **be** resolved by the effect of rotation to a great extent. Convection overshoot aids in resolving the problem of shallow CZ base position but does not affect clearly the surface helium abundance. Thus the CZ base radius of models with convection overshoot are consistent with the seismically inferred value. This reflects that rotation and convection overshoot may be important in the evolution of the Sun. Moreover, rotation plays an important role in the formation of the extended main-sequence turnoff of intermediate-age massive star clusters (Yang et al. 2013a,b); and convection overshoot plays an essential role in explaining some of characteristics of solar-like oscillations of stars (Yang et al. 2015). These indicate that the effects of rotation and convection overshoot should **not be** ignored in the evolutions of stars.

Although the rotating AGSR model can reproduce the seismically inferred sound-speed and density profiles and the CZ base radius, the neutrino fluxes calculated from this model are not in agreement with those predicted by BP04 (Bahcall & Pinsonneault 2004) and SSeM (Couvidat et al. 2003; Turck-Chièze et al. 2004; Turck-Chièze & Couvidat 2011). Moreover, the total angular momentum of  $3.85 \times 10^{48} \text{ g cm}^2 \text{ s}^{-1}$  of AGSR is too high. Turck-Chièze et al. (2011) suggested that the effects of magnetic field must be considered during the solar life. We consider the effects of magnetic pressure, magnetic energy, and magnetic mixing. The surface He abundance and neutrino fluxes are significantly improved by the effects of magnetic field.

In this work, we constructed dynamical solar models with the AGS09 mixtures in which the effects of enhanced diffusion, rotation, convection overshoot, and magnetic fields were included. We obtained two models: AGSR and AGSM that almost restore agreement with helioseismology. Compared to GS98 SSM, AGSR can reproduce the CZ base radius, the sound-speed and density profiles. The surface helium abundance of about



0.2393 of this model is  $2.6 \sigma$  away from the seismically inferred value of Basu & Antia (2004). The position of the CZ base of AGSM agrees with the seismically inferred value at the level of  $1 \sigma$ . The surface helium abundance of 0.2445 of AGSM agrees with the seismic value at the level of  $1.1 \sigma$ . The density profile of this model is as good as that of GS98M. The sound-speed profile of AGSM matches very well that inferred in Basu et al. (2009) between 0.1 and  $0.6 R_{\odot}$ . The bump of the sound speed mainly appears between  $0.63$  and  $0.71 R_{\odot}$ . The relative difference of the sound speed between AGSM and the Sun,  $\delta c/c$ , is less than 0.0058 in the tacholine. Moreover, the observed separation ratios  $r_{02}$  and  $r_{13}$  are almost reproduced by AGSM; the initial helium abundance of AGSM is in agreement with  $0.273 \pm 0.006$  given by Serenelli & Basu (2010) at the level of  $1 \sigma$ .

The  $^8\text{B}$  neutrino flux predicted by AGSM agrees with the detected one and the prediction of SSeM at the level of about  $1 \sigma$ . The fluxes of  $pp$ ,  $pep$ , and  $^7\text{Be}$  neutrinos computed from AGSM are not far from the detected ones and the predictions of BP04 and SSeM. The improvement in the sound-speed and density profiles and the CZ radius mainly derives from the effects of the enhanced diffusion and overshooting which are dependent of the dynamical processes, while the improvement in the surface helium abundance and neutrino fluxes basically comes from the effects of the dynamical processes. Although the GS98 SSM performs much better than the low-Z models as a whole, the agreement between the low-Z models and seismic and neutrino results is improved by the effects of the dynamical processes.

The author thanks the anonymous referee for helpful comments which help the author improve this work, and the support from the NSFC 11273012, 11273007, 11503039, and the Fundamental Research Funds for the Central Universities.

## REFERENCES

Adelberger, E. C., Austin, S. M., Bahcall, J. N. et al. 1998, *Rev. Mod. Phys.*, 70, 1265

Ahmed, S. N., Anthony, A. E., Beier, E. W. et al. 2004, *PhRvL*, 92, 1301

Antia, H. M., & Basu, S. 2005, *ApJ*, 620, L129

Asplund, M., Grevesesse N., Sauval, A. J., Allende Prieto, C., & Kiselman, D. 2004, *A&A*, 417, 751

Asplund, M., Grevesesse N., Sauval, A. J., Allende Prieto, C., & Blomme, R. 2005, *A&A*, 431, 693 (AGS05)

Asplund, M., Grevesse, N., Sauval, A., & Scott, P. 2009, *ARA&A*, 47, 481 (AGS09)

Badnell, N. R., Bautista, M. A., Butler, K., Delahaye, F., Mendoza, C., Palmeri, P., Zeppen, C. J., Seaton, M. J. 2005, *MNRAS*, 360, 458

Bahcall, J. N., Pinsonneault, M. H., & Basu, S., 2001, *ApJ*, 555, 990

Bahcall, J. N., & Pinsonneault, M. H. 1992, *Rev. Mod. Phys.*, 64, 885

Bahcall J. N., Pinsonneault M. H., & Wasserburg G. J. 1995, *Rev. Mod. Phys.*, 67, 781

Bahcall, J. N., & Pinsonneault, M. H. 2004, *Phys. Rev. Lett.*, 92, 121301

Bahcall, J. N., Serenelli, A. M., & Pinsonneault, M. H. 2004, *ApJ*, 614,464

Bahcall, J. N., Basu, S., Pinsonneault, M. H., & Serenelli, A. M. 2005, *ApJ*, 618, 1049

Bahcall, J. N., Serenelli, A. M., & Basu, S. 2006, *ApJS*, 165, 400

Basu, S., & Antia, H. M. 1997, *MNRAS*, 287, 189

Basu, S., Antia, H. M. 2008, *PhR*, 457, 217

Basu, S., Chaplin, W. J., Elsworth, Y., New, R., Serenelli, A. M. 2009, *ApJ*, 699, 1403

Basu, S., & Antia, H. M. 2004, *ApJ*, 606, L85

Bellini, G. Benziger, J. Bick, D. et al. 2011, *PhRvL*, 107, 141302

Bellini, G. Benziger, J. Bick, D. et al. 2012, *PhRvL*, 108, 51302

Bi, S. L., Li, T. D., Li, L. H., Yang, W. M. 2011, *ApJL*, 731, 42

Caffau, E., Ludwig, H.-G., Bonifacio, P., Faragiana, R., Steffen, M., Freytag, B., Kamp, I., Ayres, T. R. 2010, *A&A*, 514, A92

- Castro, M., Vauclair, S., Richard, O. 2007, *A&A*, 463, 755
- Chaplin, W. J., Christensen-Dalsgaard, J., Elsworth, Y., et al. 1999a, *MNRAS*, 308, 405
- Chaplin, W. J., Elsworth, Y., Howe, R., et al. 1996, *Sol. Phys.*, 168, 1
- Chaplin, W. J., Elsworth, Y., Isaak, G. R., Miller, B. A., & New, R. 1999b, *MNRAS*, 308, 424
- Christensen-Dalsgaard, J., Gough, D. O., & Thompson, M. J. 1991, *ApJ*, 378, 413
- Couvidat, S., Turck-Chièze, S., & Kosovichev, A. G. 2003, *ApJ*, 599, 1434
- Duez, V., Mathis, S., Brun, A. S., & Turck-Chièze, S. 2009, 259, 177
- Duez, V., Mathis, S., & Turck-Chièze, S. 2010, *MNRAS*, 402, 271
- Ferguson, J. W., Alexander, D. R., Allard, F. et al. 2005, *ApJ*, 623, 585
- García, R. A., Salabert, D., & Ballot, J. et al., 2011, *JPhCS*, 271, 012049
- García, R. A., Turck-Chièze, S., Jiménez-Reyes, S. J., Ballot, J., Pallé, P. L., Eff-Darwich, A., Mathur, S., Provost, J. 2007, *Sci.*, 316, 1591
- Grevesse, N., & Sauval, A. J. 1998, in *Solar Composition and Its Evolution*, ed. C. Fröhlich, et al. (Dordrecht: Kluwer), 161 (GS98)
- Gruzinov, A. V., & Bahcall, J. N. 1998, *ApJ*, 504, 996
- Guenther, D. B., Dermarque, P., Kim, Y. C., Pinsonneault, M. H. 1992, *ApJ*, 387, 372
- Guzik, J. A., Watson, L. S. & Cox, A. N. 2005, *ApJ*, 627, 1049
- Guzik, J. A., & Mussack, K. 2010, *ApJ*, 713, 1108
- Iglesias, C., Rogers, F. J. 1996, *ApJ*, 464, 943
- Komm, R., Howe, R., Durney, B. R., & Hill, F. 2003, *ApJ*, 586, 650
- Le Penneec, M., Turck-Chièze, S., Salmon, S., Blancard, C., Cossé, P., Faussurier, G., Mondet, G. 2015, *ApJL*, 813, L42
- Li, L. H., & Sofia, S. 2001, *ApJ*, 549, 1204
- Lodders, K. 2003, *ApJ*, 591, 1220
- Lodders, K., Palme, H, Gail, H-P. 2009, *LanB*, 4, 44
- Lopes, I., & Turck-Chièze, S. 2013, *ApJ*, 765, 14
- Lopes, I., & Turck-Chièze, S. 2014, *ApJL*, 792, L35
- Marcucci, L. E., Schiavilla, R., Viviani, M., Kievski, A., & Rosati, S. 2000, *Phys. Rev. Lett.*, 84, 5959
- Montalbán, J., Miglio, A., Noels, A., Grevesse, N., Di Mauro, M. P. 2004, in *Helio- and Asteroseismology: Towards a Golden Future*, Proc. of the SOHO 14 / GONG 2004 Workshop, ed. D. Danesy (ESA SP-559; Noordwijk: ESA), 574
- Montalban, J., Miglio, A., Theado, S., Noels, A., Grevesse, N. 2006, *Commun. Asteroseismol.*, 147, 80
- Pinsonneault, M. H., Kawaler, S. D., Sofia, S., & Demarque, P., 1989, *ApJ*, 338, 424
- Proffitt, C. R., & Michaud, G. 1991, *ApJ*, 380, 238
- Rogers, F., & Nayfonov, A. 2002, *ApJ*, 576, 1064
- Roxburgh, I. W., & Vorontsov, S. V. 2003, *A&A*, 411, 215
- Schmelz, J. T., Nasraoui, K., Roames, J. K., Lippner, L. A., & Garst, J. W. 2005, *ApJ*, 634, L197
- Serenelli, A., & Basu, S. 2010, *ApJ*, 719, 865
- Serenelli, A., Basu, S., Ferguson, J., & Asplund, M. 2009, *ApJL*, 705, 123
- Serenelli, A., Haxton, W. C., Peña-Garay, C. 2011, *ApJ*, 743, 24
- Spruit, H. C. 2002, *A&A*, 381, 923
- Thoul, A. A., Bahcall, J. N., Loeb, A. 1994, *ApJ*, 421, 828
- Turck-Chièze, S., & Couvidat, S. 2011, *RPPH*, 74, 6901
- Turck-Chièze, S., Couvidat, S., Kosovichev, A. G. et al. 2001, *ApJL*, 555, L69

- Turck-Chièze, S., Couvidat, S., Piau, L., Ferguson, J., Lambert, P., Ballot, J., García, R. A., Nghiem, P. 2004, *Phys. Rev. Lett.*, 93, 211102
- Turck-Chièze, S., & Lopes, I. 2012, *RAA*, 12, 1107
- Turck-Chièze, S., Palacios, A., Marques, J. P., Nghiem, P. A. P. 2010, *ApJ*, 715, 1539
- Turck-Chièze, S., Piau, L., & Couvidat, S. 2011, *ApJL*, 731, L29
- Young, P. R. 2005, *A&A*, 444, L45
- Yang, W. M., & Bi, S. L. 2006, *A&A*, 449, 1161
- Yang, W. M., & Bi, S. L. 2007, *ApJ*, 658, L67
- Yang, W. M., & Bi, S. L. 2008, *ChJAA*, 8, 677
- Yang, W., Bi, S., & Meng, X. 2013a, *RAA*, 13, 579
- Yang, W., Bi, S., Meng, X., & Liu, Z 2013b, *ApJ*, 776, 112
- Yang, W., Tian, Z., Bi, S., Ge, Z., Wu, Y., & Zhang, J. 2015, *MNRAS*, 453, 2094
- Zahn, J. P., Talon, S., & Matias, J. 1997, *A&A*, 322, 320
- Zhang, Q., & Li, Y. 2012, *ApJ*, 746, 50
- Zhang, Q. 2014, *ApJ*, 787, L28

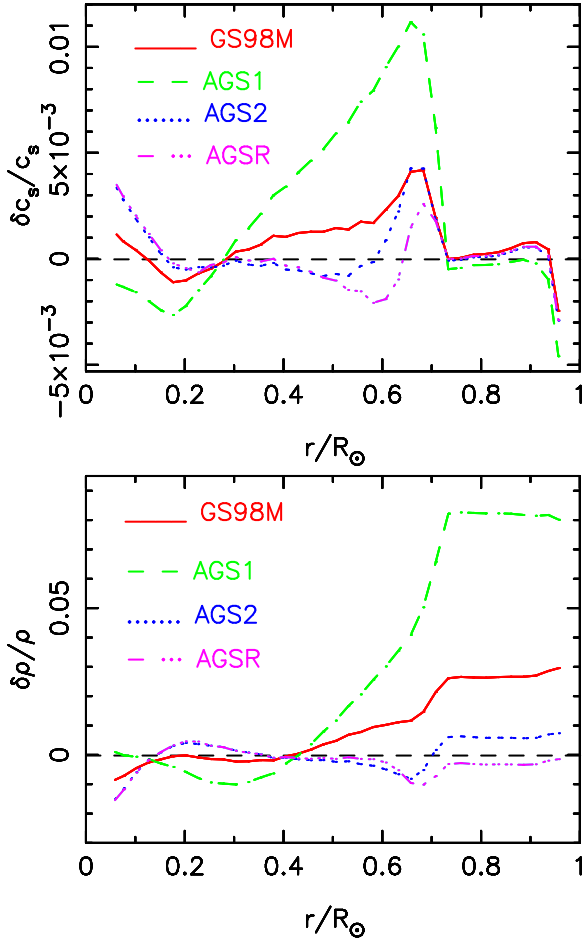


Fig. 1.— The relative sound-speed difference and density difference, in the sense (Sun-Model)/Model, between solar models and helioseismological results. The helioseismological sound speed and density are given in Basu et al. (2009).

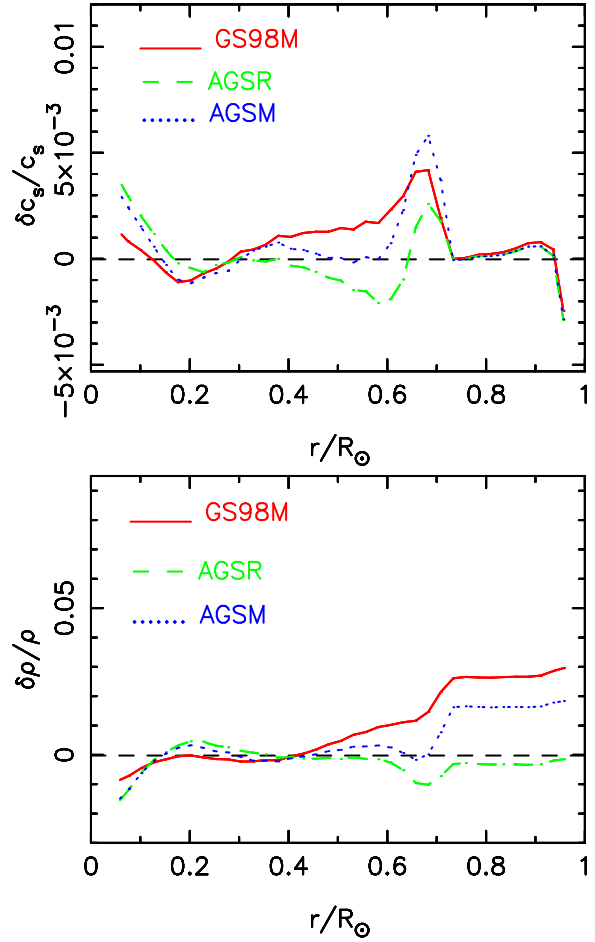


Fig. 2.— The relative sound-speed difference and density difference, in the sense (Sun-Model)/Model, between solar models and helioseismological results. The helioseismological sound speed and density are given in Basu et al. (2009).

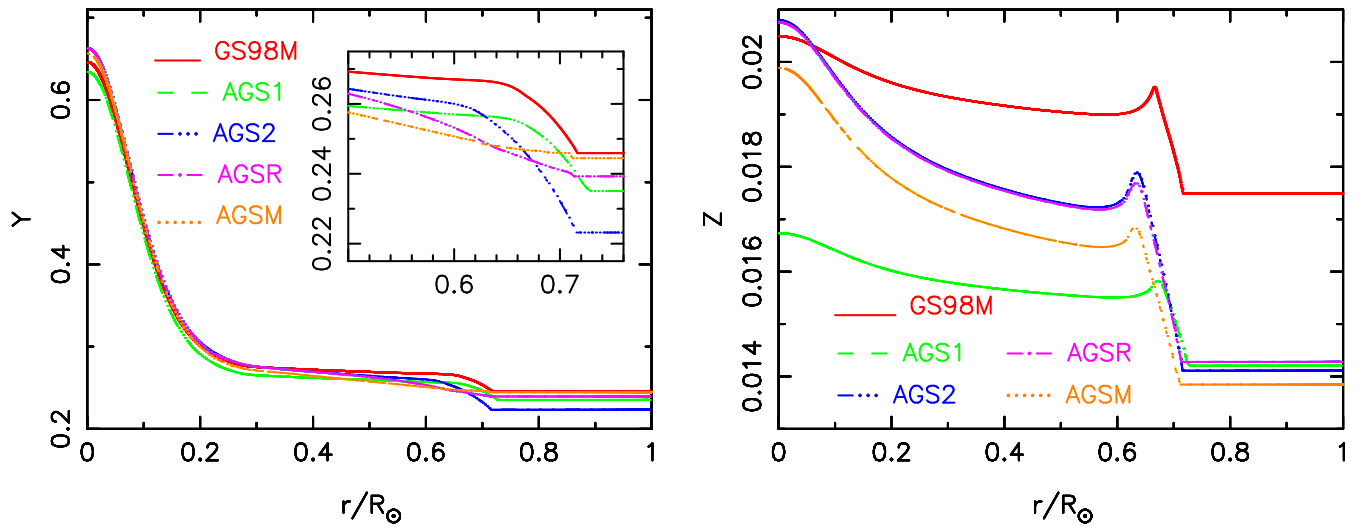


Fig. 3.— Radial distributions of helium and heavy-element mass fraction of different models.

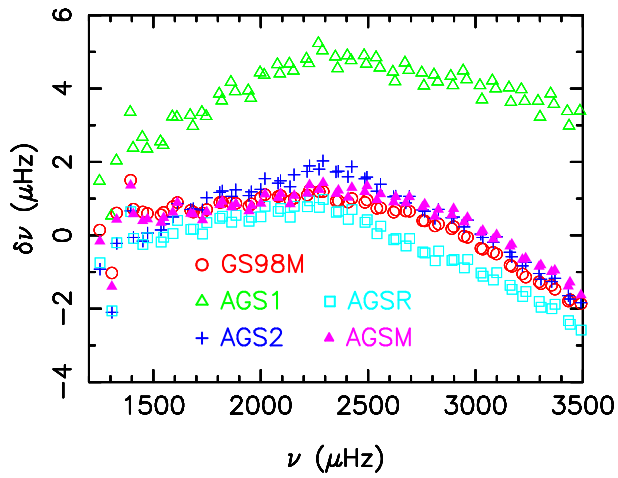


Fig. 4.— Observed minus theoretical frequency vs theoretical frequency of different models for low-degree modes. The frequencies of low-degree p-modes of the Sun are observed by GOLF & VIRGO (García et al. 2011).

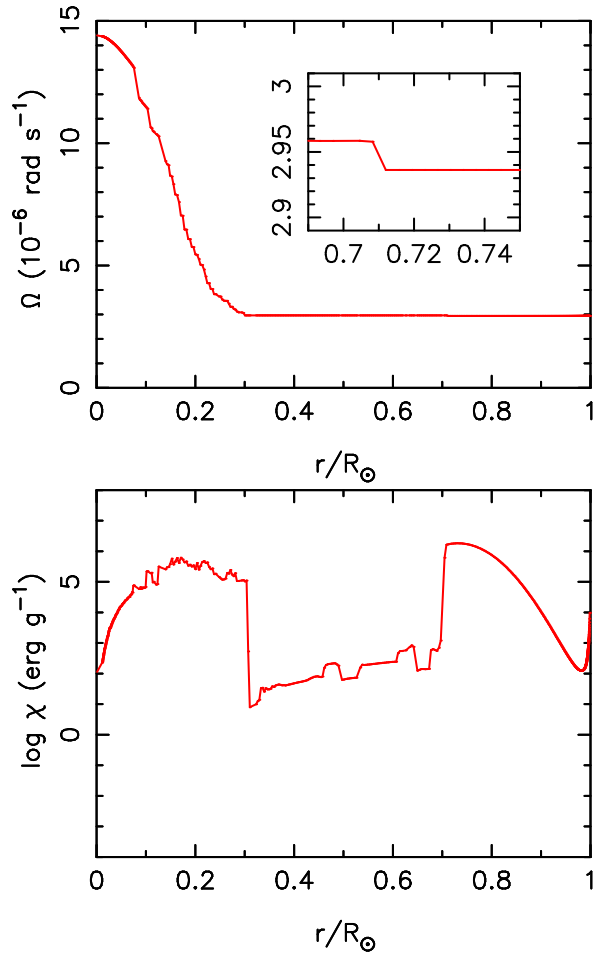


Fig. 5.— Radial distributions of angular velocity and magnetic energy density of AGSM.

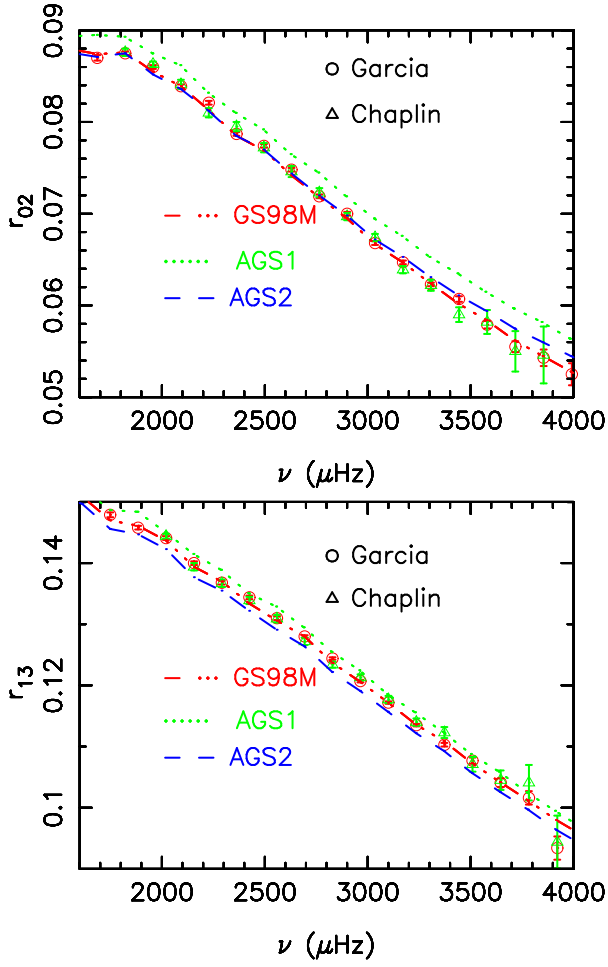


Fig. 6.— The distributions of the ratios of small to large separations,  $r_{02}$  and  $r_{13}$ , as a function of frequency. The circles show the ratios calculated from the frequencies observed by GOLF & VIRGO (García et al. 2011), while the triangles represent the ratios computed from the frequencies observed by BiSON (Chaplin et al. 1999b).

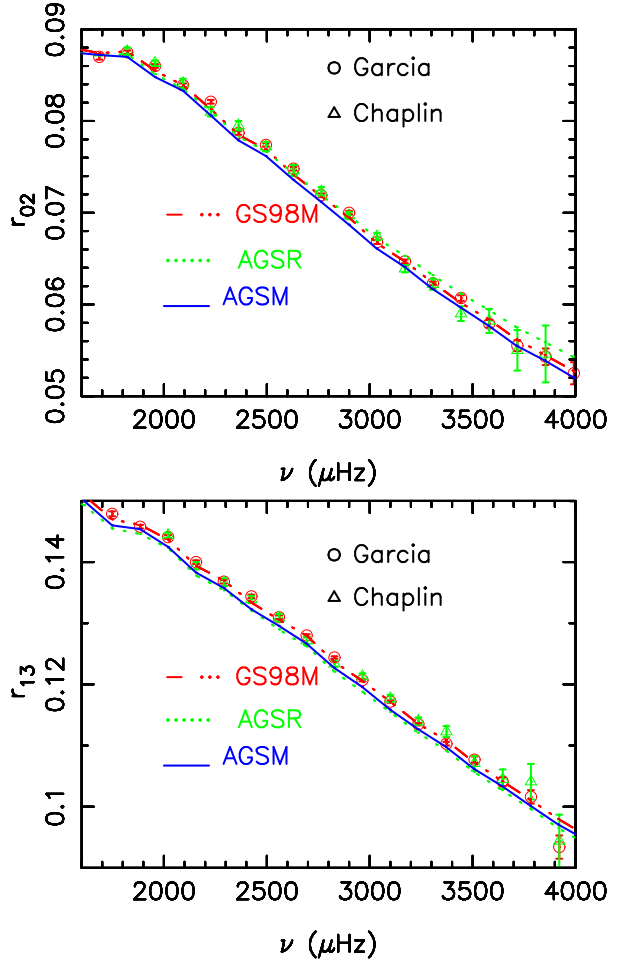


Fig. 7.— The distributions of ratios  $r_{02}$  and  $r_{13}$  as a function of frequency. The circles show the ratios calculated from the frequencies observed by GOLF & VIRGO (García et al. 2011), while the triangles represent the ratios computed from the frequencies observed by BiSON (Chaplin et al. 1999b).

Table 1: Model parameters.

Parameter	GS98M	AGS1	AGS2	AGSR	AGSM
$X_{init}$	0.70418	0.71772	0.70334	0.7034	0.7085
$Y_{init}$	0.27638	0.266397	0.27844	0.27841	0.274054
$Z_{init}$	0.01944	0.015883	0.01822	0.01819	0.017446
$\alpha$	2.213	2.1769	2.402	2.25748	2.336
$\delta_{ov}$	0	0	0	0.1	0.2
$V_{init}$ (km s <sup>-1</sup> )	0	0	0	5.8	5.8
Multiplier	1.0 <sup>a</sup> (1.0) <sup>b</sup>	1.0 (1.0)	2.0 (2.5)	2.0 (2.5)	2.0 (2.5)
$f_{\Omega}$	0	0	0	0	0.01
$f_c$	0	0	0	0	$1.0 \times 10^{-4}$
$T_c$ (10 <sup>6</sup> K)	15.78	15.65	16.00	15.99	15.91
$\rho_c$ (g cm <sup>-3</sup> )	154.64	152.14	156.39	156.38	156.01
$X_c$	0.3337	0.3492	0.3162	0.3167	0.3233
$Y_c$	0.6458	0.6341	0.6630	0.6626	0.6568
$R_{cz}/R_{\odot}$	0.716 <sup>c</sup>	0.729	0.716	0.714	0.712
$Y_s$	0.24591	0.23507	0.22317	0.23928	0.2445
$Z_s$	0.01748	0.01420	0.01411	0.01427	0.01385
$(Z/X)_s$	0.0237	0.0189	0.0185	0.0191	0.0187
$V_e$ (km s <sup>-1</sup> )	0	0	0	1.90	2.04
$J_{tot} \times 10^{48}$ (g cm <sup>2</sup> s <sup>-1</sup> )	0	0	0	3.85	2.40

<sup>a</sup>The multiplier for the diffusion coefficient of the helium;

<sup>b</sup>The multiplier for the diffusion coefficient of the heavy elements;

<sup>c</sup>Using OPAL EOS96, Bahcall et al. (2004) obtained  $R_{cz} = 0.7155 R_{\odot}$ .

Table 2: Predicted solar neutrino fluxes from models. The table shows the predicted fluxes, in units of  $10^{10}(pp)$ ,  $10^9(^7\text{Be})$ ,  $10^8(pep, ^{13}\text{N}, ^{15}\text{O})$ ,  $10^6(^8\text{B}, ^{17}\text{F})$ , and  $10^3(hep)$  cm<sup>2</sup>s<sup>-1</sup>. The BP04 is the best model of Bahcall & Pinsonneault (2004) and has the GS98 mixtures. The SSeM is the best standard model that reproduces the seismic sound speed (Couvidat et al. 2003; Turck-Chièze & Couvidat 2011). The old SSeM has high-metal abundances (Couvidat et al. 2003), but the new SSeM has the low-metal abundances (Turck-Chièze et al. 2004; Turck-Chièze & Couvidat 2011).

Source	GS98M	AGS1	AGS2	AGSR	AGSM	BP04	old SSeM	new SSeM	Measured
$pp$	5.95	6.01	5.88	5.88	5.91	5.94	5.92	....	$6.06^{+0.02(a)}_{-0.06}$
$pep$	1.40	1.43	1.38	1.38	1.39	1.40	1.39	....	$1.6 \pm 0.3^{(b)}$
$hep$	9.47	9.77	9.24	9.22	9.33	7.88	....	....	....
$^7\text{Be}$	5.11	4.72	5.60	5.57	5.33	4.86	4.85	4.72	$4.84 \pm 0.24^{(a)}$
$^8\text{B}$	5.22	4.43	6.48	6.41	5.82	5.79	4.98	$5.31 \pm 0.6$	$5.21 \pm 0.27 \pm 0.38^{(c)}$
$^{13}\text{N}$	5.46	3.91	6.47	6.42	5.71	5.71	5.77	....	....
$^{15}\text{O}$	4.83	3.39	5.88	5.82	5.13	5.03	4.97	....	....
$^{17}\text{F}$	5.59	3.89	6.88	6.82	5.99	5.91	3.08	....	....

<sup>(a)</sup>Bellini et al. (2011).

<sup>(b)</sup>Bellini et al. (2012).

<sup>(c)</sup>Ahmed et al. (2004).